ERDC/EL TN-22-3
July 2022

Organogel Synthesis Towards Electrochemical Sensing Applications

P.U. Ashvin I. Fernando, Matthew W. Glasscott[1], Garrett W. George, Gilbert K. Kosgei[2], and Lee C. Moores

PURPOSE: The purpose of this study was to synthesize a novel and tunable organogel system capable of stand-alone use with integration via electrochemical tools for the detection of aerosol particles.

BACKGROUND: Sensing via gel-based systems is a rapidly growing field. Multiple innovative physicochemical crosslinking strategies are employed to render gels with desirable properties, such as stiffness, flexibility, self-healing, biocompatibility, etc. (Ahmed 2015; Li et al. 2018). For instance, hydrogel-based systems have been utilized to generate stimuli-responsive sensors for various biomolecules (Buenger et al. 2012).

Aerosols are ubiquitous in nature but have been weaponized to carry harmful toxins (Riches et al. 2012). Thus, technologies to capture and analyze chemical content of aerosolized particles are critical to protect Soldiers from these airborne threats. For aerosol sensing applications, it is important to have a matrix capable of capturing toxins, and gels representing a suitable matrix due to their rigidity, portability, and synthetic tunability compared to liquid-based particle capture methods (Jayawardene et al. 2014). While hydrogels are easily synthesized, they tend to dry out and lose functionality over time due to the evaporation of water. This can be overcome by using organogel systems, which are fabricated using organic solvents with a lower vapor pressure than of water.

One possible sensing method to analyze chemical contents of aerosols are electrochemical sensors using Molecularly Imprinted Polymer (MIP) recognition elements. To accomplish this, ferrocenyl compounds (e.g., ferrocene methanol, ferrocene carboxylic acid) are commonly employed as reporter molecules for the indirect detection of various analytes (Fernando et al. 2020; Leibl et al. 2021). This reporter molecule is generally introduced into a milliliter solution of interest, which limits its application in aerosol-based detection platforms due to the sub-picoliter volume of aerosol particles. The goal was to incorporate ferrocene directly into an organogel matrix to provide the reporter molecule necessary to facilitate MIP-based sensing without external addition of ferrocene.

OBJECTIVE: It is crucial that the gel matrix contains supporting electrolytes for electron transfer through the gel matrix for electrochemical-based detection. Incorporation of Li-salts was pursued, demonstrating the gel matrix's tunability for the required application. In this study, an acryloyl

[1] matthew.w.glasscott@usace.army.mil
[2] gilbert.k.kosgei@usace.army.mil

US Army Corps of Engineers®

Approved for public release; distribution is unlimited.

morpholine monomer was used as it can be easily polymerized and crosslinked to fabricate gels (Gao et al. 2019).

MATERIALS AND METHODS: The reagents listed below were purchased from Millipore Sigma and used as received.

- Lithium bis-trifluoromethanesulfonimide (99.95% trace metals basis) (LiTFSI) was used as an electrolyte salt.
- Acryloyl morpholine (97%, contains 1,000 ppm monomethyl ether hydroquinone as inhibitor) (ACMOTM) was used as a water-soluble monomer.
- Poly(ethylene glycol) diacrylate (PEGDA) average M_n 250 was used as a crosslinker.
- 1-Hydroxycyclohexyl phenyl ketone (99%) (Photoinitiator 184 or PI-184) was used as a photoinitiator.
- Propylene carbonate (ReagentPlus®, 99%) (PC) was used as the solvent.
- Tetrabutylammonium hexafluorophosphate (for electrochemical analysis, ≥99.0%) TBA-PF6.

INSTRUMENTATION: A 365 nm LED light (M300L4 - 300 nm, 26 mW (Min) Mounted LED, 350 mA) was used as the light source for the polymer formation, which was coupled to a DC2200 LED driver unit for fine tunability. Both units were Thor Labs products. All electrochemical experiments were conducted using a BASi PalmSens 4 potentiostat. PStrace software was used to facilitate all experiments. Screen-printed electrodes characterized by a gold working electrode (3 mm diameter), a silver-silver chloride (Ag/AgCl) paste reference electrode, and a carbon ink counter electrode were obtained from Brewer Scientific. Cyclic voltammograms were carried out at a scan rate of 100 mV/s with a 1 mV increment. Impedance measurements were conducted from 50,000-0.1 Hz with 10 points per decade at a DC voltage of 0 V vs Ag/AgCl. Uncompensated resistance was estimated using the high-frequency portion of the Bode plot and assuming a Randles circuit.

SYNTHETIC PROCEDURE: The concentration of LiTFSI was 0.5 M, which resulted in the highest conductivity (Yang et al. 2019). The precursor solution was prepared by sequential addition of 1 ml of the monomer solution, then 0.1 mol% (with respect to monomer) of PEGDA 250 or PEGDA 700 crosslinker solution, 1 mol% (with respect to monomer) of PI-184, and 3 ml of 0.5 M Li-salt dissolved in Propylene carbonate solution (Figure 1). The solution was then mixed in an amber vial and vigorously magnetically stirred for approximately 30 min at room temperature, followed with vortex stirring for 1 min. Then, the precursor solution was transferred to a custom mold and cured using ultraviolet light irradiation (365 nm) for 1 – 2 hr to obtain organogel ionic conductors. In addition, 0.5 M $TBAPF_6$ was added when needed into the precursor solution to enhance the ionic conductivity and simulate a supporting electrolyte system.

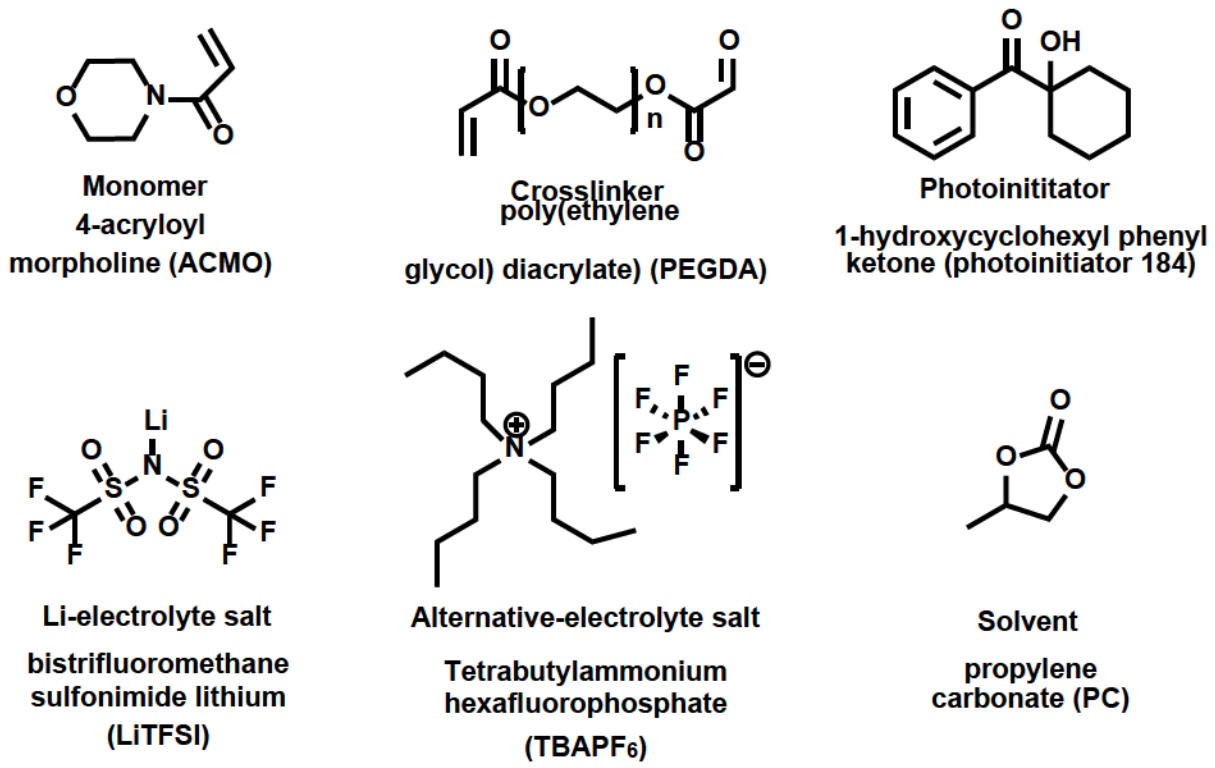

Figure 1. Molecular structure of reagents used in the organgel synthesis.

RESULTS AND DISCUSSION: The curing efficiency of the organogel synthesized is dependent on several factors such as lamp intensity, wavelength, mold thickness, and exposure timeframe. Because the 365 nm light utilized during the experiment had low power output (i.e., intensity), the curing time in this procedure exceeded the literature procedure (Gao et al. 2019). After optimizing the procedure, ferrocene methanol was added as a redox reporter extending the organogel functionality toward aerosol sensing. The synthesis was attempted several times to optimize the material, revealing the importance of using very small amounts of crosslinker to avoid decreases in structural flexibility from increased crosslinking density. The organogels were cured in an easily releasable silicon mold. The cured organogels with and without ferrocene methanol embedded in the matrix were evaluated electrochemically to monitor their electron transfer properties (Figure 2).

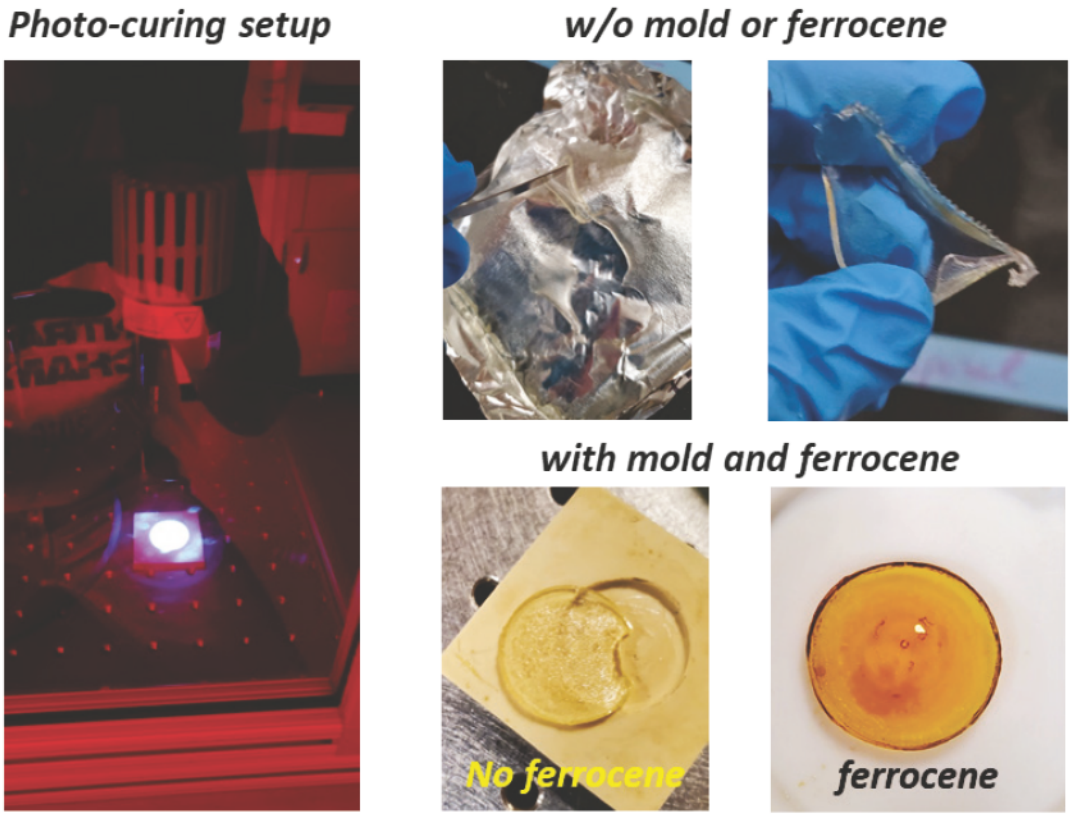

Figure 2. Experimental setup for the photo-curing process, organogels fabricated with and without the mold, and after addition of ferrocene methanol.

After the preliminary fabrication using molds, organogels were cured directly onto screen-printed electrodes printed on polyethylene terephthalate (PET) (Figure 3). As PET is non-reactive, the gel does not react with the PET surface. The screen-printed electrodes consist of three planar electrodes, a disk-shaped working electrode composed of gold, a quarter-round reference electrode composed of silver-silver chloride paste, and comparably larger three-quarter-round counter electrode composed of carbon. Initially, control gels were fabricated on the electrode without ferrocene, hence the absence of a yellow color in the images. Electrical conductance was visualized by observing the illumination of a LED, which is attached to two separated organogels pieces.

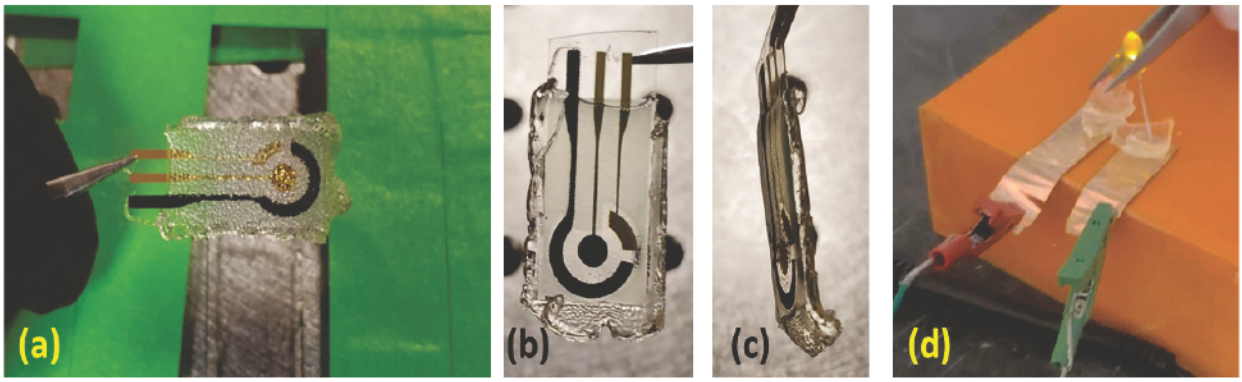

Figure 3. (a), (b), (c) – the physical appearance of organogels fabricated on top of the screen-printed electrode and (d) – electrical conductance through two separated organogels.

However, these organogels have a theoretically relatively high ohmic resistance, prompting the addition of Li-salts/TBA-salts to increase the gel conductivity. The initial cyclic voltammogram (CV) scans suggested the presence of electrical conductance within the organogel matrix with and without supporting electrolyte salts. These electrochemical signals show oxidative and reduction processes. The oxidative processes produce positive current, and reductive have produced negative current. Scanning positive from 0 V vs. Ag/AgCl shows an initial peak at ca. 0.5 V versus Ag/AgCl, which is likely gold oxidation (based on the subsequent reduction peak in the cathodic sweep, *vide infra*) (Figure 4).

Oxidation of the polymer then begins at ca. 0.85 V versus Ag/AgCl. Scanning negative shows a cathodic peak at ca. -0.1 V versus Ag/AgCl attributed to the reduction of gold oxide based on the high degree of peak symmetry (Burke and Nugent 1997), followed by a peak at ca. -0.8 V versus Ag/AgCl attributed to oxygen reduction, then reduction of the polymer itself at ca. -1 V versus Ag/AgCl. The oxidation peak at -0.1 V is possibly related to the unreacted monomer fraction, and this hypothesis will be examined in future studies via repeated voltametric cycling. Notably, the potentials referenced against Ag/AgCl may be subject to drift due to the lack of a true equilibrium at the reference electrode, which may explain peak shifting in Figure 4b (Niu et al. 2020). pH changes at the electrode surface due to the high currents used in the experiments may have also affected peak positions in Figure 4b (Niu et al. 2020). Because these electrochemical processes are occurring in a unique semi-solid-state matrix, it is difficult to assign any given peak with certainty, and future experiments will attempt to positively identify the observed peaks.

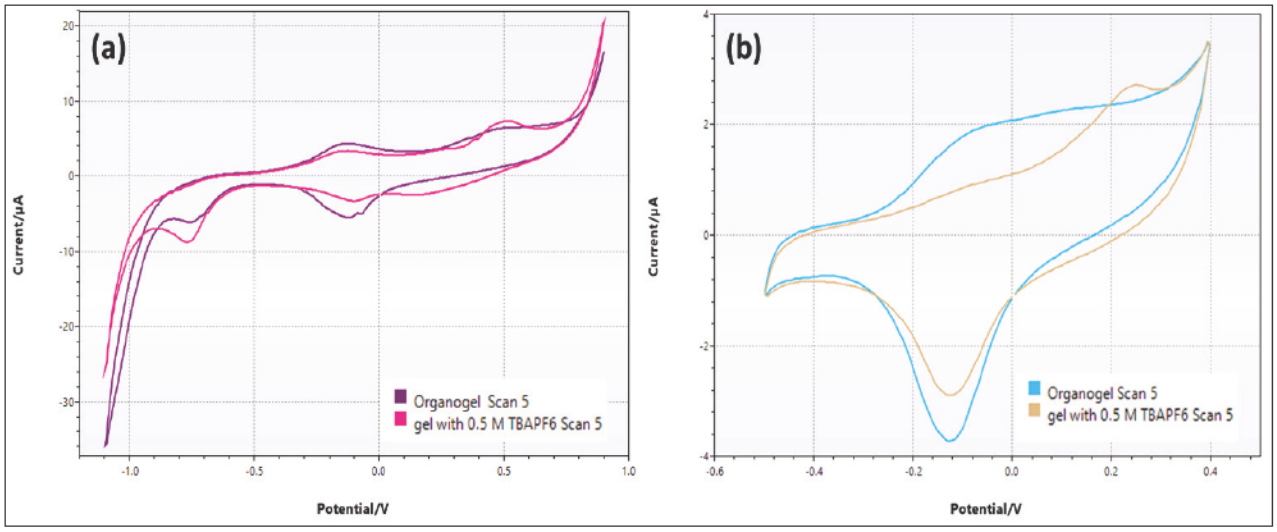

Figure 4. (a) CV of organogels with and without TBAPF6 salt and (b) CV of the same gels but at a minimized potential window.

Electrochemical impedance spectroscopy was conducted to obtain the uncompensated resistance, R_u, which indicates the resistance between the reference and the working electrodes, with and without $TBAPF_6$ (Figure 5). Since the distance between the reference and working electrodes was consistent on the screen-printed electrodes employed, the uncompensated resistance offers a qualitative indication of the solution/polymer conductivity. The organogels resulted in an R_u of 750 Ω without the supporting electrolyte salt, and when the supporting electrolyte was included in the gel matrix, R_u decreased to 540 Ω, suggesting the addition of supporting electrolyte salts increased the overall ionic conductivity within the organogel matrix.

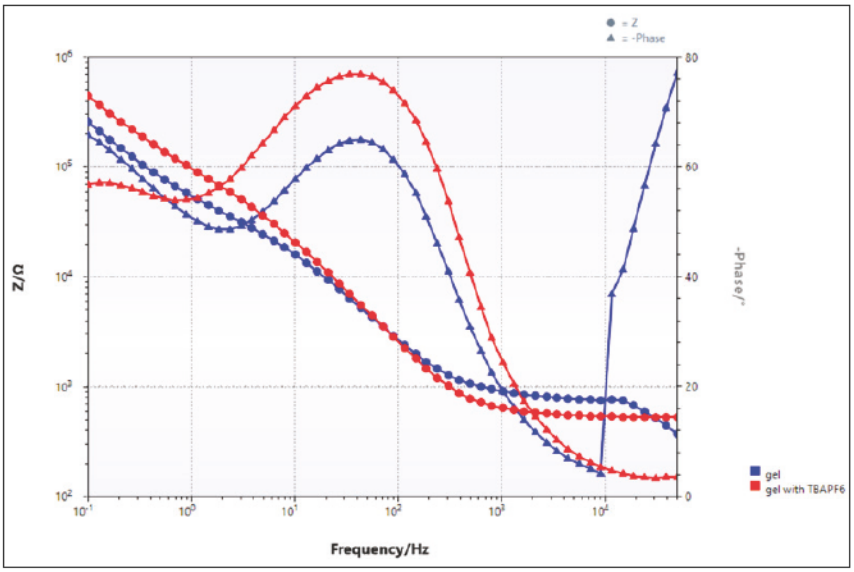

Figure 5. Bode plot with and without TBAPF6 within the organogels matrix.

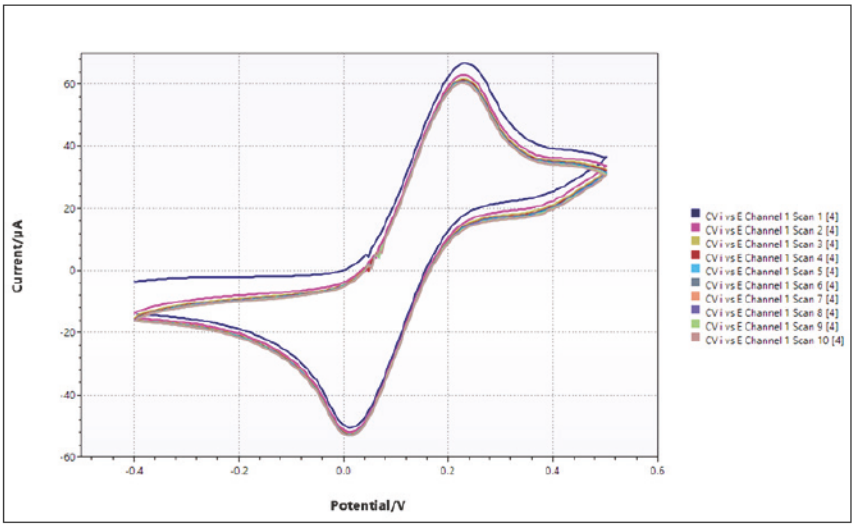

Figure 6. Multiple CV scans of the organogels with the ferrocene methanol within the gel matrix.

Finally, the ferrocene methanol was added into the organogels matrix to measure how the ferrocene behaves within the matrix of the organogel. Scanning positive from 0 V versus Ag/AgCl, ferrocene methanol is oxidized to produce a current peak at ca. 0.25 V versus Ag/AgCl. Small peaks are observed at higher potentials which are consistent with those observed in the background (Figure 4a). Scanning negative from 0.5 V versus Ag/AgCl, a reduction peak at ca. 0 V versus Ag/AgCl is observed, corresponding to the reduction of the ferrocenium methanol formed during the oxidation process back to ferrocene methanol (Figure 6). Ferrocene methanol appears to be freely diffusing within the polymer matrix based on the asymmetric "duck" shape of this voltammogram, though significant peak splitting (200 mV) indicates some additional impedance. Assuming the uncompensated resistance is ca. 600 Ω and the peak current is 60 µA, a peak distortion of 36 mV would be expected based on Ohm's law, making the total expected peak splitting 95 mV (Nernstian contribution of 59 mV plus *iR* drop contribution) (Elgrishi et al. 2018). Over 100 mV of peak splitting is unaccounted for; meaning electromigration of the ferrocenium methanol cation is likely contributing to the peak splitting (Batchelor-Mcauley et al. 2015). These effects may be more clearly established by varying the concentration of ferrocene methanol in future studies. However, the ferrocene behaved well within the matrix as indicated by the stable CV obtained over ten scans. Further studies should be undertaken to determine if the ferrocene degrades within the matrix over time, and the next goal will be to covalently attach ferrocene to the gel matrix.

SUMMARY: The synthesized organogel matrix appears to show appropriate electron transfer due to the presence of Li-salts. Furthermore, the thickness of the gel can easily be controlled using a specific mold. The short-term stability of the gel (5 voltammetric cycles) may allow this system to be used as a stand-alone passive detection matrix. The non-covalently attached ferrocene showed a good signal electrochemically and the CV stability indicates ferrocene methanol is stable over several hours. The critical information acquired from this work will be used to facilitate attachment of ferrocenyl moieties directly to the organogel matrix. Future work to covalently attach the ferrocene to the gel matrix to avoid diffusion during experiments is currently being pursued and additional experiments will be conducted to check the stability of the gel matrix. The thickness of

the gel will be altered to suit the requirement of aerosol sensing, and model aerosol sensing using evaporative organic solvents, such as chloroform, will be tested to understand aerosol diffusion within the gel matrix.

POINTS OF CONTACT: For additional information, contact Dr. P U Ashvin Iresh Fernando (payagala.a.fernando@erdc.dren.mil), Dr. Matthew Glasscott (matthew.w.glasscott@usace.army.mil), or Dr. Gilbert Kosgei (gilbert.k.kosgei@usace.army.mil).

REFERENCES

Ahmed, E. M. 2015. "Hydrogel: Preparation, characterization, and applications: A review." *J. Adv. Res.* 6 (2): 105–121. https://doi.org/10.1016/j.jare.2013.07.006.

Batchelor-Mcauley, C., E. Kätelhön, E. O. Barnes, R. G. Compton, E. Laborda, and A. Molina. 2015. "Recent advances in voltammetry." *ChemistryOpen*, 4 (3): 224–260. https://doi.org/10.1002/open.201500042.

Buenger, D., F. Topuz, and J. Groll. 2012. "Hydrogels in sensing applications." *Buenger, D.; Topuz, F.; Groll, J. Hydrogels Sens. Appl. Prog. Polym. Sci.* 37 (12): 1678–1719. https//doi.org/10.1016/j.progpolymsci.2012.09.001.

Burke, L. D., and P. F. Nugent. 1997. "The Electrochemistry of Gold: I. The redox behaviour of the metal in aqueous media." *Gold Bull.*, 30 (2): 43–53. https://doi.org/10.1007/BF03214756.

Elgrishi, N., K. J. Rountree, B. D. McCarthy, E. S. Rountree, T. T. Eisenhart, and J. L. Dempsey. 2018. "A practical beginner's guide to cyclic voltammetry." *J. Chem. Educ.*, 95 (2): 197–206. https://doi.org/10.1021/acs.jchemed.7b00361.

Fernando, P. U. A. I., M. W. Glasscott, K. Pokrzywinski, B. M. Fernando, G. K. Kosgei, and L. C. Moores. 2020. "Analytical methods incorporating molecularly imprinted polymers (MIPs) for the quantification of microcystins: A mini-review." *Crit. Rev. Anal. Chem.* 0 (0): 1–15. https://doi.org/10.1080/10408347.2020.1868284.

Gao, Y., L. Shi, S. Lu, T. Zhu, Y. Li, H. Bu, G. Gao, and S. Ding. 2019. "Highly stretchable organogel ionic conductors with extreme- temperature tolerance." *Chem. Mater.* 31: 3257–3264. https://doi.org/10.1021/acs.chemmater.9b00170.

Jayawardene, I., P. E. Rasmussen, M. Chenier, and H. D. Gardner. 2014. "Evaluating the capabilities of aerosol-to-liquid particle extraction system (ALPXS)/ICP-MS for monitoring trace metals in indoor air." *J. Air Waste Manag. Assoc.* 64 (9): 1028–1037. https://doi.org/10.1080/10962247.2014.921255.

Leibl, N., K. Haupt, C. Gonzato, and L. Duma. 2021. "Molecularly imprinted polymers for chemical sensing: A tutorial review." *Chemosensors* 9 (6): 1–19. https://doi.org/10.3390/chemosensors9060123.

Li, X., Q. Sun, Q. Li, N. Kawazoe, and G. Chen. 2018. "Functional hydrogels with tunable structures and properties for tissue engineering applications." *Front. Chem.* 6 (OCT): 1–20. https://doi.org/10.3389/fchem.2018.00499.

Niu, S., S. Li, Y. Du, X. Han, and P. Xu. 2020. "How to reliably report the overpotential of an electrocatalyst." *ACS Energy Lett.*, 5 (4): 1083–1087. https://doi.org/10.1021/acsenergylett.0c00321.

Riches, J. R., R. W. Read, R. M. Black, N. J. Cooper, and C. M. Timperley. 2012. "Analysis of clothing and urine from moscow theatre siege casualties reveals carfentanil and remifentanil use." *J. Anal. Toxicol.* 36 (9): 647–656. https://doi.org/10.1093/jat/bks078.

Yang, Y., D. M. Davies, Y. Yin, O. Borodin, J. Z. Lee, C. Fang, M. Olguin, Y. Zhang, E. S. Sablina, X. Wang, C. S. Rustomji, and Y. S. Meng. 2019. "High-efficiency lithium-metal anode enabled by liquefied gas electrolytes." *Joule* 3 (8): 1986–2000. https://doi.org/10.1016/j.joule.2019.06.008.

NOTE: *The contents of this technical note are not to be used for advertising, publication, or promotional purposes. Citation of trade names does not constitute an official endorsement or approval of the use of such products.*